Langmuir

Article

pubs.acs.org/Langmuir

Hexadecylamine Adsorption at the Iron Oxide−Oil Interface

Mary H. Wood,[†] Rebecca J. L. Welbourn,[†] Timothy Charlton,[‡] Ali Zarbakhsh,[§] M. T. Casford,[†] and Stuart M. Clarke*,[†]

[†]Department of Chemistry and BP Institute, Cambridge University, Cambridge CB2 1EW, United Kingdom

[‡]ISIS, Rutherford Appleton Laboratory, Didcot OX11 0QX, United Kingdom

[§]School of Biological and Chemical Science, Queen Mary University of London, Joseph Priestly Building, Mile End Road, London E1 4NS, United Kingdom

ABSTRACT: The adsorption behavior of a model additive, hexadecylamine, onto an iron surface from hexadecane oil has been characterized using polarized neutron reflectometry, sum-frequency generation spectroscopy, solution depletion isotherm, and X-ray photoelectron spectroscopy (XPS). The amine showed a strong affinity for the metal surface, forming a dense monolayer at relatively low concentrations; a layer thickness of 16 (±3) Å at low concentrations, increasing to 20 (±3) Å at greater amine concentrations, was determined from the neutron data. These thicknesses suggest that the molecules in the layer are tilted. Adsorption was also indicated by sum-frequency generation spectroscopy and XPS, the latter indicating that the most dominant amine−surface interaction was via electron donation from the nitrogen lone pair to the positively charged iron ions. Sum-frequency generation spectroscopy was used to determine the alkyl chain conformation order and orientation on the surface.

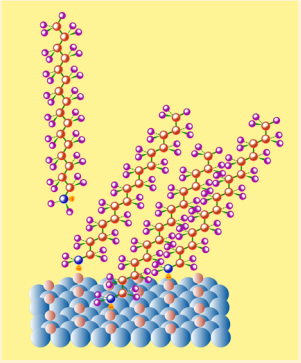

INTRODUCTION

Amines and their derivatives are frequently added to engine oils for anticorrosive or lubricating purposes. However, the nature of their interactions with the surfaces that they protect remains unclear, particularly when used in conjunction with other additive species, such as fatty acids or zinc dialkylthiophosphates (ZDDPs). For example, it remains open to debate whether they directly bind to the surface or are used rather to improve the binding of other additives.[1,2] Such questions remain unresolved because of the inability of traditional methods to study these additives *in situ* and to construct a molecular-level model of the additive interaction with the surface.

In this work, we combine a number of surface-specific and surface-sensitive techniques to address the detailed adsorption behavior and surface molecular structure of a model additive, 1-hexadecylamine adsorbed from hexadecane onto an iron surface. Zhu et al. demonstrated that 1-hexadecylamine in a tetradecane system between two mica surfaces shows similar performance to a commercial automatic transmission fluid in terms of the "hard-wall thickness" and rheological effects under shear.[3] The amine molecules were reported to form monolayers at concentrations as low as 0.1 wt % in the oil, with film thicknesses of around 18 Å, separated by a small layer of oil and excess amine, as measured using a surface force balance.

Neutron reflectometry (NR) is a well-established technique for the study of the air/liquid and solid/liquid interfaces.[4−8] In this approach, the generated reflectivity profile, obtained by reflecting a neutron beam at grazing angles close to the critical angle, has features that depend upon structural parameters of the adsorbed species, such as layer composition, thickness, and roughness. Here, in a modification of the standard approach, polarized neutron reflectometry (PNR) has been used;[9] neutrons polarized either parallel (+) or antiparallel (−) ("up"- or "down"-spin) to an external magnetic field interact differently with magnetic materials, such as iron (magnetic moment, $\mu = 2.2\ \mu_B$). For magnetic materials that are magnetized in the plane of the surface using an external field, the neutron refractive index, n, is dependent upon the neutron spin polarization. The measured reflectivity, $R^{\pm}$, is spin-dependent, and the refractive index must be written as a combination of the nuclear ($n_{nuclear}$) and magnetic ($n_{magnetic}$) contributions

$$n_{\pm} = n_{nuclear} \pm n_{magnetic} = 1 - \left(\frac{N\lambda^2}{2\pi}\right)(b \pm C\mu)$$

where N is the number density, C is a constant ($0.265 \times 10^{-12}\ \mu_B\ cm^{-1}$), b is the scattering length, and μ is the moment per atom.

When two separate reflectivity profiles are acquired for the same sample using up- and down-spin neutrons successively, two independent data sets are obtained from the same sample. This additional information is important when extracting the structural model of the interface by data fitting, because the number of possible models that can be fitted to both sets of data is significantly reduced. The scattering power of each layer at the interface is quantified in the scattering length density

Received: May 14, 2013
Revised: October 3, 2013
Published: October 9, 2013

   dx.doi.org/10.1021/la4018147 | *Langmuir* 2013, 29, 13735−13742

(SLD). The SLDs for the materials used in this work are given in Table 1.

Table 1. SLD Values of Materials Used[a]

	ρ ($\times 10^{-6}$, Å^{-2})		ρ ($\times 10^{-6}$, Å^{-2})
Si	2.27	SiO_2	4.58
Fe (up-spin)	12.99	Fe (down-spin)	3.05
Fe_2O_3 (up-spin)	7.19	Fe_2O_3 (down-spin)	3.93
$C_{16}D_{34}$	6.72	$C_{16}H_{33}NH_2$	−0.26

[a]Values for iron and iron oxide depend upon the polarization of neutrons used.

The model-fitting technique is a recognized method used to analyze reflectivity data. The interfacial region is divided into a finite number of layers, each characterized by a thickness, d, scattering length density, ρ, and roughness, from which the reflectivity is calculated using the optical matrix method. A flat background is generally added to each point, and instrumental resolution may also be taken into consideration in the calculations.

The calculated reflectivity is then compared to the experimental data, and the goodness of the fit is evaluated in terms of χ^2:

$$\chi^2 = \sum_N \left\{ \frac{(R_f - R_m)^2}{\sigma^2} \right\}$$

where N is the number of data points, R_f and R_m are the fitted and measured reflectivities, respectively, and σ is the error bar associated with the measured reflectivity.[10] The value of χ^2 is minimized by the least-squares routine. Each parameter (number of layers, thickness, etc.) can be kept fixed or varied, and the reflectivity is calculated from the model until the value for χ^2 has reached a minimum. The optimum fitted parameters combine to give the SLD profile of the sample, which represents the variation in composition perpendicular to the interface. From the fitted reflectivity data, the adsorbed amount in the layer, Γ, may be calculated using the following formula:[5]

$$\Gamma = \frac{\rho_{layer} d}{N_A \sum_i b_i}$$

where $\sum_i b_i$ is the sum of the coherent scattering lengths for each species and N_A is Avogadro's number.

The reflectivity data cannot generally be directly inverted to give a unique structural solution because of the usual phase problem between reciprocal and real space. When fitting the model, we aim to find structural solutions consistent with the experimental data (within the experimental error), but often more than one structural model may be consistent with a given set of data. This results in an effective error bar for the experimentally determined structural parameters.

We have previously characterized the adsorption behavior of palmitic acid, the carboxylic acid analogue to the amine studied here, using PNR.[11] A monolayer of the acid, with a layer thickness of 16 (±5) Å was identified, with an additional diffuse layer in the surrounding oil. The amount of adsorbed acid was estimated from the scattering length density of the fitted layer, which indicated that full monolayer coverage was attained by a concentration of 1000 ppm (3.9×10^{-3} mol dm^{-3}).

In sum-frequency generation spectroscopy (SFG), another surface-specific technique, a vibrational spectrum of the interfacial molecules, is obtained by spatially and temporally overlapping a fixed visible and tunable infrared (IR) laser beam to generate an output laser beam with frequency equal to the sum of the two incident beams. The high energy of the laser beams gives rise to nonlinear optical effects, in particular the second-order susceptibility, $\chi^{(2)}$, which will only have a non-zero value in a non-centrosymmetric environment. Hence, importantly for surface studies, there is no signal from the bulk material, and only the interface, where the symmetry is broken and $\chi^{(2)}$ has a non-zero value, is specifically investigated.[12]

The SFG technique can be used to extract several interfacial parameters, including the tilt angle of various moieties within the molecule (most frequently methyl or methylene groups) to the surface normal, molecular conformation, and polar orientation. These may be determined by variation of the polarization combinations of the incident and reflected beams.[13] The non-resonant contribution present for metal surfaces can be used to unambiguously identify the absolute orientation of a molecule on a surface.

Depletion isotherms are used to quantitatively determine the adsorbed amount of a species as a function of the solution concentration. In this technique, solutions of different initial adsorbate concentrations are added to a high-surface-area powdered substrate and allowed to equilibrate. Adsorption leads to a reduction of the adsorbate concentration in the solution, which may then be measured, in this case, using Fourier transform infrared (FTIR) spectroscopy. In many cases, the data can be best interpreted in terms of the Langmuir isotherm, where adsorption increases rapidly until monolayer coverage is attained.[14]

X-ray photoelectron spectroscopy (XPS) was used to characterize the nature of the iron surface to determine the metal surface composition and oxidation state of the iron. The interfacial amine was also probed using this technique.

EXPERIMENTAL SECTION

Materials. The iron oxide substrates used for PNR and SFG experiments were sputtered to a thickness of 200 Å onto a polished silicon substrate, (111) orientation, (n) type, with a diameter of 55 mm and thickness of 5 mm, at the Helmholtz Zentrum, Berlin, Germany, using reactive magnetron sputtering.[15] The iron oxide powder was purchased from Sigma-Aldrich (>99% purity, 69.7% Fe, determined by titration), and Brunauer−Emmett−Teller (BET) surface area (determined by N_2 adsorption fitted to the BET isotherm equation) was 4.15 m^2 g^{-1}. Hexadecylamine [98.1%, determined by gas chromatography (GC)] and dodecane (97.1%, determined by GC) were also purchased from Sigma-Aldrich. Deuterated hexadecane [99.2%, determined by proton nuclear magnetic resonance (^{1}H NMR)] was purchased from Cambridge Isotopes Laboratories, Inc., and deuterated hexadecylamine (99.2%, determined by GC) was purchased from QMX Laboratories. They were used without further purification.

Solution Depletion Isotherm. A solution depletion isotherm was measured by tumbling samples of 10 mL of hexadecyl-d_{33}-amine in dodecane (over the concentration range of 0.0−3.5×10^{-3} mol dm^{-3}) with iron oxide powder (0.5 g). Samples were allowed to equilibrate over 24 h, before centrifuging to separate the solid from the supernatant, before analysis of the final concentration by integration of peaks in the C−D stretching region of the IR spectra compared to a set of calibration standards.

PNR. The PNR experiments were conducted on the PolRef instrument at ISIS, Rutherford Appleton Laboratory, U.K. The sample setup is depicted in Figure 1. Briefly, a pulsed neutron beam from the spallation target is directed toward the sample at grazing angles and collimated by slits. Polarized neutrons were used to provide extra contrasts; polarization was achieved by the use of a transmission

dx.doi.org/10.1021/la4018147 | Langmuir 2013, 29, 13735−13742

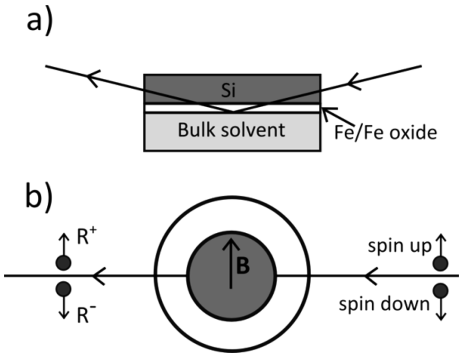

Figure 1. Experimental setup for the PNR: (a) side view schematic of the neutron reflectometry cell and (b) top view of the polarized neutron reflection. B is the magnetic field across the substrate.

polarizer, current sheet, and mirror polarizer. The neutron polarization was maintained by a series of permanent magnets (approximately 0.03 T) along the flight path. The reflection data were collected at three incident angles of 0.25°, 1.5°, and 2.5° by tilting the sample in the beam. A ^{3}He single detector was used. Further details of the instrument may be found in ref 16.

The deuterated oil was pipetted directly onto a roughened silicon surface, and the sputtered iron surface [cleaned using ultraviolet (UV)/ozone] was placed over this, separated from the base by a polytetrafluoroethylene (PTFE) O-ring, to create a thin oil layer and held in place by means of a heavy weight. The lower silicon surface was roughened to minimize unwanted reflection from this surface and additional background which might arise. This is depicted schematically in Figure 1a).

The iron substrate was characterized by PNR under air and in hexadecane-d_{34}. Solutions of hexadecylamine in the deuterated hexadecane were then added to the experimental cell in increasing concentrations, and reflectivity profiles were measured with both polarization states.

SFG. The SFG measurements were taken using an EKSPLA picosecond spectrometer (30 ps pulses at 20 Hz) at the Department of Chemistry at the University of Cambridge. The same iron-sputtered silicon substrates were used as for the PNR experiments and also cleaned using UV/ozone, after which no hydrocarbon residue remained. PPP and SSP (where the order is sum-frequency, visible, and IR) polarization combinations over the C−H stretching regions (2800−3000 cm^{-1}) were used. Although the N−H stretching region (3500−3300 cm^{-1}) was examined, no peak of significant intensity was observed and reference to the FTIR and Raman spectra of the amine showed overlap of only one peak at 3400 cm^{-1}, which had significantly lower intensity in the Raman compared to the C−H stretches. PPP spectra were also recorded for the oppositely deuterated system, i.e., hexadecyl-d_{33}-amine in protonated hexadecane, over both the C−H and C−D regions (2000−2300 cm^{-1}). A co-propagating geometry was used, with angles of 53° and 60° to the surface normal for the IR and visible laser beams, respectively. The spectra were normalized to the product of the IR and visible beam intensities using the EKSPLA normalization facility.

XPS. XPS measurements were taken at the NEXUS laboratory in Newcastle using the AXIS Nova XPS spectrometer. Small silicon wafers, 1 × 1 cm, were sputtered with iron using magnetron sputtering and cleaned for 30 min using UV/ozone. Both a bare substrate, i.e., under air, and a substrate treated with a sample of 4.25 × 10^{-3} mol dm^{-3} hexadecylamine in dodecane before being allowed to dry were analyzed, with three measurements taken from each sample to ensure representative data. Fe 2p and C 1s spectra were recorded from the bare substrate to characterize the oxide layer and cleanliness of the surface, respectively, and N 1s spectra were additionally recorded for the sample treated with the amine sample, to assess the N−surface interactions, if any, resulting from the presence of the nitrogen-containing additive.

RESULTS AND DISCUSSION

Solution Depletion Isotherm. An isotherm of hexadecyl-d_{33}-amine measured using the depletion method is given in Figure 4. The data exhibit a rapid rise in adsorption at low concentrations before reaching a plateau of approximately 3 × 10^{-6} mol m^{-2} at higher concentrations. This adsorption profile is in good agreement with a Langmuir adsorption model.[14] BET measurements of the powder give a specific surface area of 4.15 m^2 g^{-1}. Hence, the adsorption at the plateau in the isotherm corresponds to each amine molecule occupying 55 Å^2 on the substrate surface. This is reasonable given that the amine headgroup surface area is expected to be about 20 Å^2,[17] allowing for space to accommodate slightly bulkier alkyl chains.

The most common cleavage plane of the iron oxide (α-Fe_2O_3) surface is the hexagonal (0001) plane, with a unit cell size of 5 Å (as reported by Shaikhutdinov et al.[18]) between the uppermost iron atoms on the surface. Considering the size of the amine molecule, an adsorption model in which each of these Fe^{3+} sites is occupied seems implausible given the extent of crowding this would entail; if each site were occupied, the area per molecule would be 21.7 Å^2, assuming a perfect homogeneous surface across the entire powder sample. A more disperse model (e.g., with alternate sites occupied) therefore seems more probable.

Adsorption at the solid/solution interface is an exchange process and can be described by a number of models, particularly those of Everett.[19] However, where the adsorbate adsorbs strongly this adsorption may be approximated by the Langmuir model.

PNR. Figure 2a presents the neutron reflection data from the substrate under deuterated hexadecane compared to the data from the surface when exposed to 1.25 × 10^{-3} mol dm^{-3} hexadecylamine in deuterated hexadecane. The figure shows data obtained with both up- and down-spin neutron polarizations, clearly demonstrating the pronounced difference in reflectivity obtained for each, most markedly in the down-spin profiles. The iron-sputtered substrate was initially measured under air and then under the deuterated solvent to identify and characterize the metal and oxide layers present. The up-spin data exhibit a series of fringes, the spacing of which are inversely related to the thicknesses of the surface layers. The gradients of the reflectivity curves are determined by roughnesses at each interface. From a careful fitting of these data using the Polly software, these parameters were found and are shown in Table 2. The up- and down-spin data were fitted simultaneously. The iron layer thickness of 202 Å corresponded to that estimated by XRR data provided by the Helmholtz Zentrum, Berlin, Germany, where the substrates were sputtered.

The magnetic behavior of the iron and iron oxide layers is also contained in the reflectivity data and can be estimated by fitting. Here, the magnetic moment, μ, of the oxide layer (μ = 2.0 μ_B) was intermediate between Fe_2O_3 (non-magnetic, μ = 0.0 μ_B) and Fe_3O_4 (magnetic, μ = 4.1 μ_B), suggesting that the layer consists of a mixture of the two oxides. Examples of mixtures of such oxides have been reported for the sputtered iron layers in the literature.[20]

The addition of increasing concentrations of hexadecylamine in hexadecane-d_{34} led to changes in the reflectivity profiles generated, indicating that the amine molecules were interacting with the iron surface and adsorbing. The greatest changes were seen in the down-spin data, as expected. In Figure 3, the

dx.doi.org/10.1021/la4018147 | Langmuir 2013, 29, 13735−13742

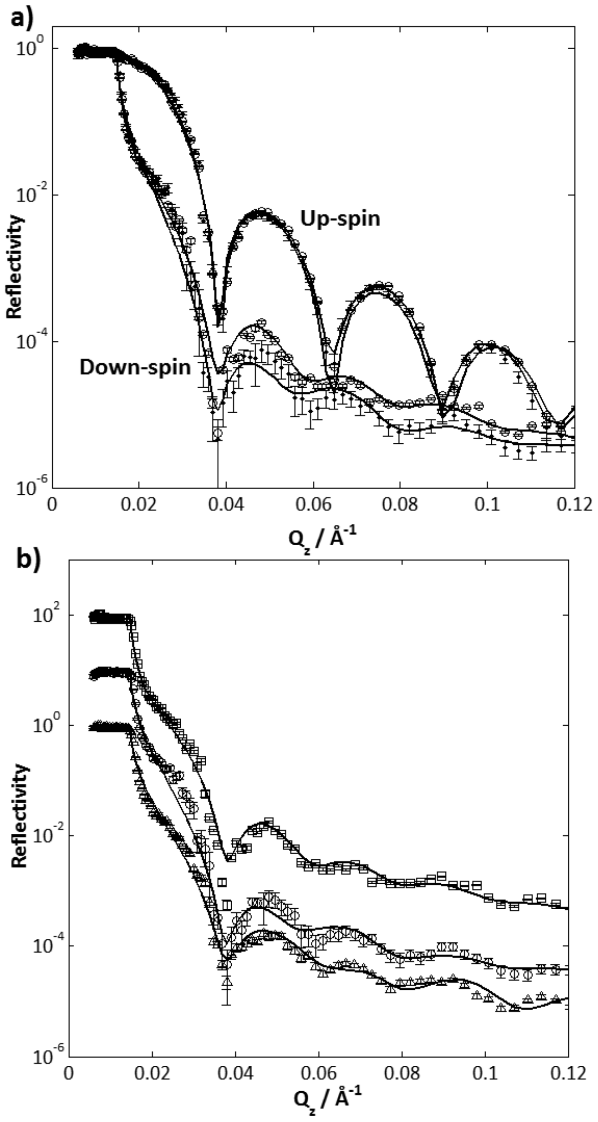

Figure 2. (a) Reflectivity data obtained with both up- and down-spin neutrons for the bare substrate under dodecane (○) and with the addition of 1.25 × 10^{-3} mol dm^{-3} amine in deuterated solvent (●). (b) Down-spin reflectivity curves for solvent only (□), with the addition of 1.25 × 10^{-3} mol dm^{-3} amine (○), and with the addition of 4.25 × 10^{-3} mol dm^{-3} amine (△) in the deuterated solvent. For clarity, each of these profiles is shifted by a factor of 10. The reflectivity axes are on a logarithmic scale.

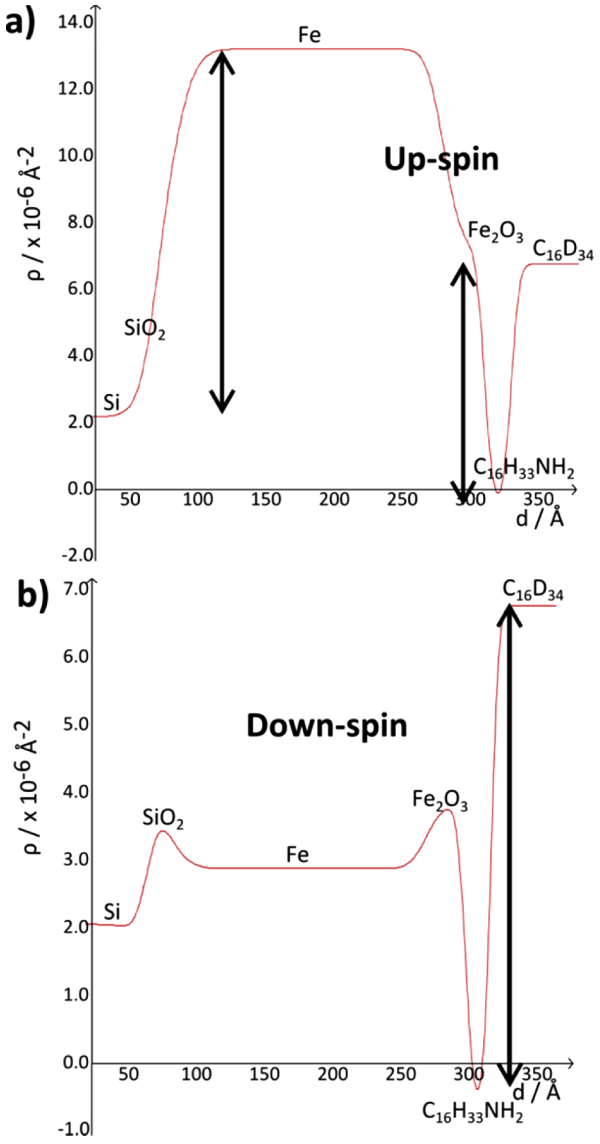

Figure 3. (a) For the up-spin neutrons, the contrast relating to the thin adsorbed layer is swamped by that between the iron and underlying silicon, (b) whereas there is only one major contrast for the down-spin neutrons (shown by the bold arrows).

simulated SLD profile is depicted schematically along the vertical *z* axis passing through the interface. For the down-spin simulation, there is only one major contrast, related to the adsorbed layer, whereas the presence of a larger contrast (between the iron and silicon) for the up-spin simulation causes the up-spin neutrons to be less sensitive to changes in the adsorbed layer.

Table 2. Fitted Layer Parameters and Fitted ρ Values for the Increasing Amine Concentrations with Their Corresponding Adsorbed Amounts

layer	thickness (Å)	roughness (Å)	$[amine]_{initial}$ (mol dm^{-3})	fitted ρ value (×10^{-6}, $Å^{-2}$)	coverage (%)	adsorbed amount (×10^{-6}, mol m^{-2})
Si		12	1.03 × 10^{-4}	5.00	25.7	2.26
SiO_2	10	9.4	4.18 × 10^{-4}	4.02	39.4	4.05
Fe	202	15.6	1.25 × 10^{-3}	3.82	42.1	4.41
Fe_2O_3	30	10	4.25 × 10^{-3}	3.16	51.4	5.46
amine layer, low concentrations (1 and 4 × 10^{-4} mol dm^{-3})	16 (±3)	4.9				
amine layer, high concentrations (1 and 4 × 10^{-3} mol dm^{-3})	20 (±3)	5.0				

dx.doi.org/10.1021/la4018147 | *Langmuir* 2013, 29, 13735−13742

Examples of the down-spin data are shown in Figure 2b where reflectivity profiles obtained with down-spin neutrons for the two highest concentrations, 1.25×10^{-3} and 4.25×10^{-3} mol dm^{-3} amine, are compared to that for the substrate under the deuterated solvent only. Models fitted to the experimental data for each concentration gave a layer thickness for the adsorbed amine of 16 (±3) Å at the two lower concentrations (1.03×10^{-4} and 4.18×10^{-4} mol dm^{-3}) and 20 (±3) Å as the concentration was increased to 1.25×10^{-3} and 4.25×10^{-3} mol dm^{-3} (the error in the layer thickness was estimated from the minimum and maximum thicknesses over a range of SLDs that could be fitted to the data). The variation in layer thickness with concentration (from 16 to 20 Å) is of the order of the experimental uncertainty, and hence any changes on layer thickness are rather modest. The extended hexadecylamine chain length is expected to be 21.5 Å,[21] suggesting that the measured layer thickness is reasonable. The difference is proposed to arise from one or more of several possibilities; the amine molecules may sit tilted on the surface or may extend into the porous oxide surface, or conformation disorder in the chains may exist, producing a slightly thinner layer than the fully extended chain. At higher concentrations, the increased adsorption appears to have led to some reorientation of the alkyl chains.

The scattering length densities of the amine layer were also fitted and found to decrease with an increasing amine concentration. It is expected that the ratio of amine to solvent in the adsorbed layer will increase with more amine adsorption, and the SLD should therefore tend from that of hexadecane-d_{34}, 6.717×10^{-6} Å^{-2}, toward that of hexadecylamine, -0.260×10^{-6} Å^{-2}, as observed. The fitted values are shown in Table 2, also expressed as percent coverage of the two components (deduced from the amine/solvent ratio needed to attain the fitted scattering length density), along with the corresponding adsorbed amounts (calculated assuming the layer thickness of 16 Å and molecular volumes of 5.127×10^{-28} and 4.867×10^{-28} m^3 for the amine and solvent, respectively; these were calculated from molecular weights of 241.46 and 259.97 g mol^{-1} and bulk densities of 0.782 and 0.887 g mL^{-1} for the amine and solvent, respectively).

The concentration dependence of the reflection indicates that the amine shows a relatively high affinity for the iron surface even at low concentrations, reaching a coverage of around 50% (in terms of the amine/solvent ratio calculated from the fitted SLD) at saturation. The adsorbed amounts determined by PNR have been plotted alongside the depletion isotherm data in Figure 4. While the curve shapes are very similar, with the half-maximum concentrations being the same for both sets of data, the PNR data show a plateau value significantly higher than that of the depletion isotherm, giving an area per amine molecule of around 30 Å^2, a value somewhat less than that given by the solution isotherms outlined above. This difference in behavior may potentially arise from a number of effects. These include the surface roughness of the iron oxide layer in the neutron reflection experiments, because the adsorbed amounts are calculated assuming a completely flat surface. However, as reported above, the surface roughness is significant (approximately 10 Å), and hence the actual surface area is larger than the geometric area of the wafer. Simple calculations based on the experimentally determined roughness indicate that this effect can account for the difference in adsorption between the isotherm and neutron reflection approaches. Another potential contributing factor may be differences in the nature and composition of the oxide layer for the powder and sputtered thin film.

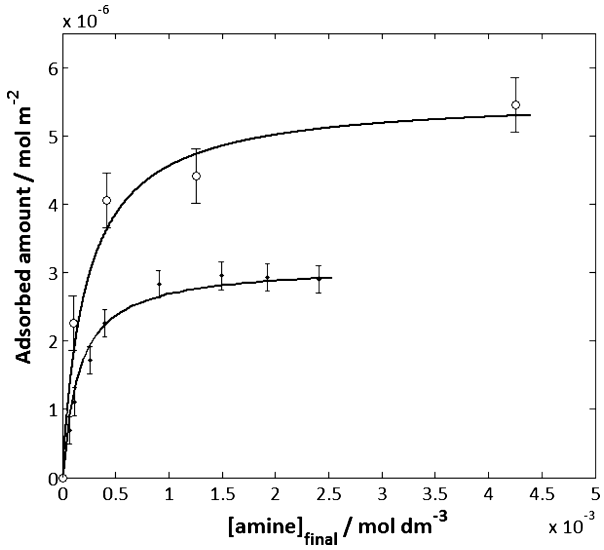

Figure 4. Comparison of the PNR (○) and depletion isotherm (●) data. Values calculated from the PNR data have assumed a completely flat surface. The calculated Langmuir isotherms are also shown (lines).

SFG. Figure 5a shows the SFG spectra taken over the C−H stretching region (2800−3000 cm^{-1}) for hexadecylamine adsorbed onto iron from hexadecane-d_{34} with the two polarization combinations PPP and SSP. There are five resolvable bands in the PPP spectrum, which are assigned to the methylene symmetric stretch (d^+) at 2847 cm^{-1} and its associated Fermi resonance at ca. 2900 cm^{-1}, the methyl symmetric stretch (r^+) at 2872 cm^{-1} with its Fermi resonance at 2936 cm^{-1}, and the methyl antisymmetric stretch (r^-) at 2964

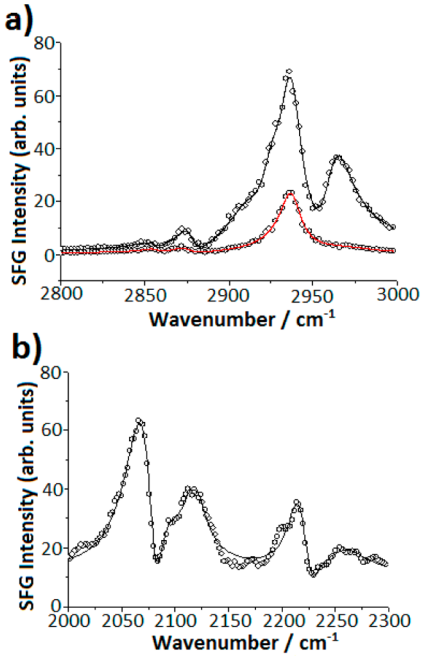

Figure 5. (a) SFG spectra over the C−H stretching region for PPP (top) and SSP (bottom) combinations. (b) PPP SFG spectrum of hexadecyl-d_{33}-amine in hexadecane. The amine concentration in both cases is 4.25 × 10 mol dm^{-3}.

dx.doi.org/10.1021/la4018147 | Langmuir 2013, 29, 13735−13742

cm^{-1}. It is immediately apparent that the methyl Fermi resonance is disproportionately strong in the spectra for both polarization combinations. Because the Fermi resonance draws intensity from the fundamental, its intensity should be no greater than equivalent to the fundamental band with which it is associated. In this case, the same effect has previously been reported by Zhang et al. for a mild steel surface on which octadecane thiol has been self-assembled.[22] In their paper, the increased intensity of the Fermi resonance is attributed to the presence of iron oxide. Because our surface is predominately composed of an oxide layer, as will be demonstrated by the XPS data discussed subsequently, this strengthening of the Fermi resonance band may also be attributed to the iron oxide film. Because interpretation of the SFG spectra relies heavily on the relative intensities of the methyl and methylene bands, the PPP spectrum of deuterated hexadecylamine in the CD stretching region was also recorded (Figure 5b). This spectrum is markedly different from that observed in the CH region, being free from any distortion in band intensities arising from the Fermi resonance. This region is dominated by the methyl stretching bands at 2070, 2123, and 2217 cm^{-1}, corresponding to r^+, r^+_{Fr}, and r^-, respectively, with only two small shoulders apparent at 2098 and 2197 cm^{-1}, corresponding to the d^+ and d^- bands, respectively.[23]

From both qualitative inspection of the spectra and comparison of the modeled spectral intensities, it is clear that the methylene symmetric stretching peaks (d^+, at 2846/2098 cm^{-1}) in the PPP spectra are of almost negligible intensity compared to the peaks that correspond to the terminal methyl group stretches (at 2871/2070, 2935/2123, and 2964/2117 cm^{-1} for the r^+, r^+_{Fr}, and r^- peaks, respectively, in the CH and CD regions). This occurs when the alkyl chain conformational order is predominately all trans and the methylene modes become locally centrosymmetric and, hence, SFG-inactive, and it is therefore concluded that, although a small number of gauche defects are present, the adsorbed layer shows a high degree of conformational order.[24]

This conclusion concerning the conformational order in the alkyl chains is supported by the work of Miranda et al.,[25] who report the SFG spectra of dioctadecyl dimethyl ammonium chloride (DOAC) from solvents of varying polarity onto quartz. For polar solvents, a high level of disorder was observed, but when a nonpolar solvent of comparable molecular length to DOAC was used, hexadecane, the monolayer formed was well-ordered. The authors attribute this increased ordering to interdigitation of the solvent molecule with the adsorbate to form a tightly packed layer. The fitted SLD values observed in our neutron data also indicate that a significant proportion of solvent is present in the monolayer; it seems probable therefore that a similar process of interdigitation occurs here.

SFG spectra recorded in the CH region for the deuterated amine in hexadecane failed to produce any significant spectra for hexadecane. This is most likely due to a combination of the reduced IR intensity on the metal surface because of absorption by the bulk oil and the presumed near all-trans conformational order of the interdigitated hexadecane, which would result in a centrosymmetric and, therefore, SFG-inactive hexadecane layer.

The polar orientation of the molecules on the surface has been inferred from a comparison of the spectra presented here to spectra reported in the literature of ODT on mild steel, in which the adsorbed monolayer has a known orientation;[22] the signals attributed to methyl group stretches all appear as peaks with a modeled phase of 43° in close agreement with the 45° previously reported,[22] suggesting that the terminal methyl groups are pointing away from the surface,[12] and hence, the adsorbed layer sits with the amine headgroup oriented toward the iron surface, a result that is supported by the XPS data that show evidence of a nitrogen adsorption peak.

The tilt angle of the terminal methyl group to the surface normal was calculated by comparison of the ratio of symmetric and antisymmetric peak intensities in the PPP spectra to the theoretically simulated value derived from the method proposed by Zhang et al.,[22] found according to

$$I_{p,SF} = \varepsilon_0 c(|L_x \sum_{j}^{x,y,z} \sum_{k}^{x,y,z} \varepsilon_0 \chi^{(2)}_{xjk} K_j E^{I}_{p,vis} K_k E^{I}_{p,IR}|^2 + |L_z \sum_{j}^{x,y,z} \sum_{k}^{x,y,z} \varepsilon_0 \chi^{(2)}_{zjk} K_j E^{I}_{p,vis} K_k E^{I}_{p,IR}|^2)$$

where L and K are the nonlinear and linear Fresnel factors, respectively, $\chi^{(2)}$ is the second-order susceptibility, and $E_{p/s}$ is the surface electric field for the p- or s-polarized light. Because $\chi^{(2)}$ can be directly related to the tilt angle, θ, this permits the plotting of a curve of the ratio of intensities for the two peaks as a function of θ, from which the experimentally derived ratio may be used to determine the methyl tilt angle relative to the surface normal.

This approach gave a value for the methyl group inclination of 32°. However, this tilt angle should be treated as an estimate only given that the monolayer contains at least some gauche defects.

From simple geometric calculations using the layer thickness value of 20 (±3) Å at saturation determined by PNR and a chain length of 21.5 Å, a tilt angle of 22° to the surface normal is predicted.

XPS. The Fe 2p spectrum from the iron-sputtered silicon wafer is shown in Figure 6a; the broad peak at around 710 eV may be resolved into two peaks at 711.8 and 709.9 eV, which is consistent with the presence of the two types of iron oxide, Fe_2O_3 and Fe_3O_4. Many examples of peaks around this region exist for both oxides, and therefore, it is unsurprising that they merge in this instance.[26,27] This suggestion of a mixture of oxides at the surface is consistent with the fitting of the magnetic moment seen for the PNR data. A small shoulder at 706.9 eV is attributed to the presence of unoxidized iron.[26]

No change in the Fe 2p region was observed for the sample treated with amine in dodecane; this is unsurprising, because the proportion of iron affected by any reaction with the amine would be very small in comparison to the entire depth of iron analyzed (on the order of around 100 Å).

Figure 6b, the N 1s spectrum for the sample treated with hexadecylamine/hexadecane, shows a broad peak that is not evident in the untreated substrate; this may be resolved into three components, at 401.1, 399.7, and 397.2 eV (with a ratio of intensities roughly 1:6:3), which may be assigned by reference to expected peaks in various environments. The peak at 397.2 eV is presumed to result from amine that has not reacted with the surface but remains on the sample, "free amine", because the lower binding energy indicates a higher electron density than the species that give rise to the remaining peaks. We were not able to completely remove any excess solution prior to measurement, and therefore, this "free" amine is taken to represent amine that was dried onto the surface during the XPS measurements rather than amine adsorbed in the "wet" system. The peak at 399.7 eV corresponds well to

dx.doi.org/10.1021/la4018147 | Langmuir 2013, 29, 13735−13742

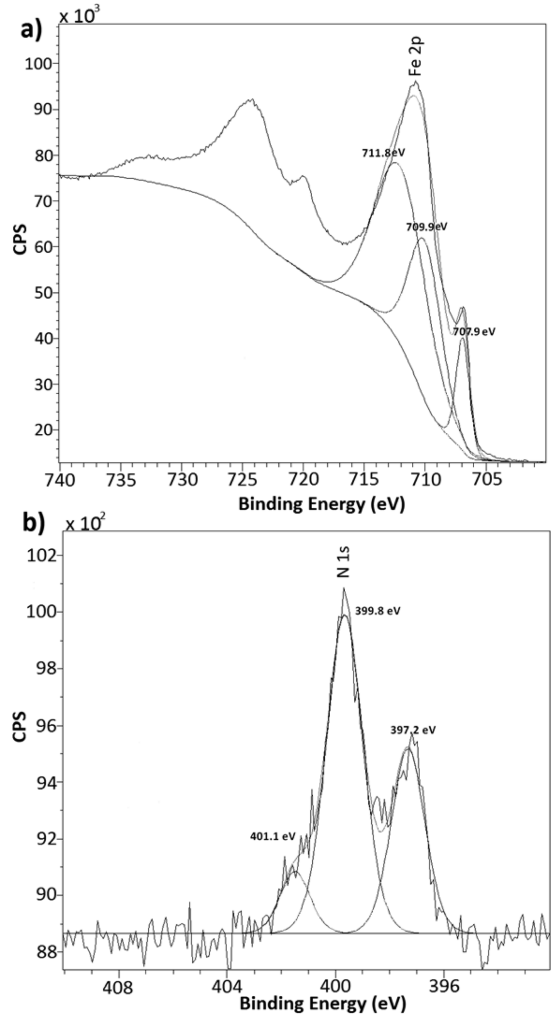

Figure 6. (a) XPS spectrum of the Fe 2p region. The peak at 711.8 eV indicates that the main oxidation state is Fe(III), with a small amount of Fe(II) at 709.9 eV, and some unoxidized iron present at 707.9 eV. (b) XPS spectrum of the N 1s region for the amine-treated wafer. The fitted lines indicate the three different nitrogen environments at the peak positions shown.

what might be expected for a nitrogen atom donating electron density to the iron surface via its lone pair (Willenbruch et al. report a value of 399.8 eV for ammonia on an iron surface[28]) and, hence, is assumed to arise from the chemisorbed amine. The smallest peak, at 401.1 eV, has a rather high energy that indicates a more positively charged amine. This may arise from the interaction with negatively charged surface oxygen atoms; Weng et al. report a value of 401.5 eV for an "oxidized N" within a CNO^- group.[29] Small water impurities present in the solvent may account for this protonation of the amine group. The low peak intensity relative to the other peaks indicates that this species would be present in far lower concentrations.

CONCLUSION

Experimental methods to characterize an iron/iron oxide surface and the adsorption behavior of an alkyl amine from oil thereupon have been presented in this work. All techniques used demonstrate the binding of the hexadecylamine species to the iron oxide surface. The XPS data indicate chemisorbed amine, where the nitrogen is donating electron density to the surface iron(III) ions. The strong affinity of the amine for the surface is also observed in adsorption isotherms using solution depletion and PNR methods, in both of which the adsorbed amount is seen to increase steeply with the concentration, resulting in a high plateau coverage. The SFG spectra demonstrate that the methylene groups are in an all-trans configuration with the polar headgroup directed toward the surface.

Several parameters that characterize the adsorbed layer were identified; from the PNR data fitting, a modest increase in layer thickness from 16 to 20 (±3) Å was observed as the amine concentration was increased, slightly above the experimental precision. The molecular tilt angle was also calculated both using this PNR value and also from consideration of the SFG peak intensity ratios. However, the latter was considered unreliable because of the unexpected enhancement of the Fermi peak intensity; therefore, the tilt angle of the methyl group is considered most likely to fall into the 30−50° range, relative to the surface normal. A depiction of the model for hexadecylamine adsorption to the iron oxide surface is shown in Figure 7. The molecules are considered to sit fully extended

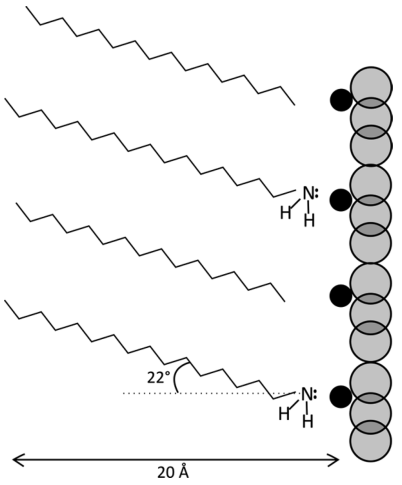

Figure 7. Proposed adsorption layer model. The light gray circles represent surface oxygen atoms, and the smaller black circles represent the topmost layer of iron atoms.

on the surface in a well-ordered layer, whereby the amine nitrogens donate electron density to the iron cations that sit on top of the iron oxide (0001) plane. From the XPS nitrogen spectra, it seems possible that a small proportion of semi-positive amine molecules that interact electrostatically with the surface oxygen atoms may also be found in the adsorbed layer.

AUTHOR INFORMATION

Corresponding Author

*E-mail: stuart@bpi.cam.ac.uk.

Notes

The authors declare no competing financial interest.

ACKNOWLEDGMENTS

The authors thank Dr. Seung Yeon Lee, University of Cambridge, for BET powder surface area measurements and Dr. Roland Steitz and Prof. Jan-Ekkehard Hoffmann at the Helmholtz Zentrum, Berlin, Germany, for sputtering the iron substrates. X-ray photoelectron spectra were obtained at the National Engineering and Physical Sciences Research Council (EPSRC) XPS User's Service (NEXUS) at Newcastle

University, an EPSRC mid-range facility. NR data were obtained on the PolRef instrument at the ISIS facility, Rutherford Appleton Laboratory (RB 1120039). Mary Wood is grateful for funding from the Oppenheimer Trust, and Becky Welbourn acknowledges funding from EPSRC and BP.

REFERENCES

(1) Klokkenburg, M.; Hilhorst, J.; Erné, B. H. Surface analysis of magnetite nanoparticles in cyclohexane solutions of oleic acid and oleylamine. *Vib. Spectrosc.* **2007**, *43*, 243−248.
(2) Szauer, T.; Brandt, A. Adsorption of oleates of various amines on iron in acidic solution. *Electrochim. Acta* **1981**, *26*, 1209−1217.
(3) Zhu, Y.; Ohtani, H.; Greenfield, M. L.; Ruths, M.; Granick, S. Modification of boundary lubrication by oil-soluble friction modifier additives. *Tribol. Lett.* **2003**, *15*, 127−134.
(4) Bohmer, M. R.; Koopal, L. K.; Janssen, R.; Lee, E. M.; Thomas, R. K.; Rennie, A. R. Adsorption of nonionic surfactants on hydrophilic surfaces. An experimental and theoretical study on association in the adsorbed layer. *Langmuir* **1992**, *8*, 2228−2239.
(5) Lu, J. R.; Thomas, R. K.; Penfold, J. Surfactant layers at the air/water interface: Structure and composition. *Adv. Colloid Interface Sci.* **2000**, *84*, 143−304.
(6) Penfold, J.; Staples, E.; Tucker, I.; Thompson, L.; Thomas, R. K. Adsorption of nonionic mixtures at the air−water interface: Effects of temperature and electrolyte. *J. Colloid Interface Sci.* **2002**, *247*, 404−411.
(7) Penfold, J.; Staples, E.; Thompson, L.; Tucker, I. The composition of non-ionic surfactant mixtures at the air/water interface as determined by neutron reflectivity. *Colloids Surf.* **1995**, *102*, 127−132.
(8) Penfold, J.; Thomas, R. K.; Lu, J. R.; Staples, E.; Tucker, I.; Thompson, L. The study of surfactant adsorption by specular neutron reflection. *Phys. B* **1994**, *198*, 110−115.
(9) Ankner, J. F.; Felcher, G. P. Polarised-neutron reflectometry. *J. Magn. Magn. Mater.* **1999**, *200*, 741.
(10) Campana, M. Ph.D. Thesis, Queen Mary University of London, London, U.K., 2013.
(11) Campana, M.; Teichert, A.; Clarke, S.; Steitz, R.; Webster, J. R. P.; Zarbakhsh, A. Surfactant adsorption at the metal−oil interface. *Langmuir* **2011**, *27*, 6085−6090.
(12) Lambert, A.; Davies, P.; Neivandt, D. Implementing the theory of sum frequency generation vibrational spectroscopy: A tutorial review. *Appl. Spectrosc. Rev.* **2005**, *40*, 103−145.
(13) Zhuang, X.; Miranda, P.; Kim, D.; Shen, Y. Mapping molecular orientation and conformation at interfaces by surface nonlinear optics. *Phys. Rev. B: Condens. Matter Mater. Phys.* **1999**, *59*, 12632−12640.
(14) Giles, C. H.; Smith, D.; Huitson, A. A general treatment and classification of the solute adsorption isotherm. *J. Colloid Interface Sci.* **1974**, *47*, 755−765.
(15) Penning, F. M.; Moubis, J. H. A. Cathode sputtering in a magnetic field. *Proc. Kon. Ned. Akad. Wetensch.* **1940**, *43*, 41−56.
(16) Charlton, T. R.; Coleman, R. L. S.; Dalgliesh, R. M.; Kinane, C. J.; Neylon, C.; Langridge, S.; Plomp, J.; Webb, N. G. J.; Webster, J. R. P. Advances in neutron reflectometry at ISIS. *Neutron News* **2011**, *22*, 15−18.
(17) Meulenberg, R. W.; Bryan, S.; Yun, C. S.; Strouse, G. F. Effects of alkylamine chain length on the thermal behaviour of CdSe quantum dot glassy films. *J. Phys. Chem. B* **2002**, *106*, 7774−7780.
(18) Shaikhutdinov, S. K.; Joseph, Y.; Kuhrs, C.; Ranke, W.; Weiss, W. Structure and reactivity of iron oxide surfaces. *Faraday Discuss.* **1999**, *114*, 363.
(19) Yang, Z.; Li, Q.; Hua, R.; Gray, M. R.; Chou, K. C. Competitive adsorption of toluene and *n*-alkanes at binary solution/silica interfaces. *J. Phys. Chem. C* **2009**, *113*, 20355−20359.
(20) Beach, G. S. D.; T, P. F.; Smith, D. J.; Crozier, P. A.; Berkowitz, A. E. New magnetic order in buried native iron oxide layers. *Phys. Rev. Lett.* **2003**, *91*, 267201.
(21) Gidalevitz, D.; Huang, Z.; Rice, Sa. Urease and hexadecylamine-urease films at the air−water interface: An X-ray reflection and grazing incidence X-ray diffraction study. *Biophys. J.* **1999**, *76*, 2797−2802.
(22) Zhang, H.; Romero, C.; Baldelli, S. Preparation of alkanethiol monolayers on mild steel surfaces studied with sum frequency generation and electrochemistry. *J. Phys. Chem. B* **2005**, *109*, 15520−15530.
(23) Kubota, J.; Kusafuka, K.; Wada, A.; Domen, K.; Kano, S. S. Time-resolved sum-frequency generation spectroscopy of methoxy and deuterated methoxy on Ni(111) using near-infrared laser pulses. *J. Phys. Chem. B* **2006**, *110*, 10785−10791.
(24) Conboy, J. C.; Messmer, M. C.; Richmond, G. L. Dependence of alkyl chain conformation of simple ionic surfactants on head group functionality as studied by vibrational sum-frequency spectroscopy. *J. Phys. Chem. B* **1997**, *101*, 6724−6733.
(25) Miranda, P. B.; Pflumio, V.; Saijo, H.; Shen, Y. R. Conformation of surfactant monolayers at solid/liquid interfaces. *Chem. Phys. Lett.* **1997**, *264*, 387−392.
(26) Brion, D. Etude par spectroscopie de photoelectrons de la degradation superficielle de FeS_2, $CuFeS_2$, ZnS et PbS à l'air et dans l'eau. *Appl. Surf. Sci.* **1980**, *5*, 133−152.
(27) Marcus, P.; Grimal, J. L. The anodic dissolution and passivation of Ni−Cr−Fe alloys studied by ESCA. *Corros. Sci.* **1992**, *33*, 805−814.
(28) Willenbruch, R. D.; Clayton, C. R.; Oversluizen, M.; Kim, D.; Lu, Y. An XPS and electrochemical study of the influence of molybdenum and nitrogen on the passivity of austenitic stainless steel. *Corros. Sci.* **1990**, *31*, 179−190.
(29) Weng, L. T.; Poleunis, C.; Bertrand, P.; Carlier, V.; Sclavons, M.; Franquinet, P.; Legras, R. Sizing removal and functionalisation of the carbon fibre surface studied by combined TOF SIMS and XPS. *J. Adhesion Sci. Technol.* **1995**, *9*, 859−871.